

Pattern-wise Transparent Sequential Recommendation

Kun Ma, Cong Xu, Zeyuan Chen, Wei Zhang, *Member, IEEE*

Abstract—A transparent decision-making process is essential for developing reliable and trustworthy recommender systems. For sequential recommendation, it means that the model can identify key items that account for its recommendation results. However, achieving both interpretability and recommendation performance simultaneously is challenging, especially for models that take the entire sequence of items as input without screening. In this paper, we propose an interpretable framework (named PTSR) that enables a pattern-wise transparent decision-making process without extra features. It breaks the sequence of items into multi-level patterns that serve as atomic units throughout the recommendation process. The contribution of each pattern to the outcome is quantified in the probability space. With a carefully designed score correction mechanism, the pattern contribution can be implicitly learned in the absence of ground-truth key patterns. The final recommended items are those items that most key patterns strongly endorse. Extensive experiments on four public datasets demonstrate remarkable recommendation performance, while statistical analysis and case studies validate the model interpretability.

Index Terms—Recommender system, sequential recommendation, interpretability, transparent model

I. INTRODUCTION

RECOMMENDER systems have been engineered to expedite the process of identifying items that align with users' interests and to do so with a high degree of precision. In recent years, how to design decision-transparent models to improve the interpretability of recommender systems has become a popular topic [1], [2], [3]. Different from traditional approaches, in addition to providing highly accurate candidate items, a good interpretable model needs to have the ability to provide compelling and easy-to-understand reasons for its recommendations [3] — how the input (i.e., interacted items) affects the output (i.e., candidate items to be recommended), which not only helps model designers to judge the rationales of the results but also contributes to improving the users' trust in the recommendation results. However, for sequential recommendation, there remain two main challenges to be solved.

- **How to simultaneously achieve performance and transparency.** To accurately capture user dynamic interests, most state-of-the-art sequential recommendation models are

Transformer-based [4], [5]. Due to their black-box nature [6], poor decision transparency is to be anticipated, thereby resulting in inadequate interpretability. While some simpler alternatives may provide slightly better transparency, they often come at the expense of recommendation performance [3], [1], [2].

- **How to move beyond point-level interpretability to union-level interpretability.** Previous similarity-based studies such as NAIS [1] and RUM [2] have made some efforts on point-level interpretability, which refers to individual items providing straightforward clues in terms of user intent. As illustrated in Figure 1, the camera provides convincing evidence for purchasing a memory card since it is a must-have accessory for a camera. Nevertheless, this is inadequate because successive purchases of similar items might indicate a stronger and more reliable interest in potential future behavior, forming union-level patterns. As the figure shows, the co-occurrence of 'phone' and 'headphone' collectively implies the user's interest in electronics, which contributes to union-level interpretability. Although more interpretable, such union-level patterns have been unexplored thus far.

In this paper, we propose PTSR, a novel Pattern-wise Transparent Sequential Recommendation model, aiming to achieve good model transparency while retaining high recommendation performance. The model extracts point-level and union-level patterns to represent the varied granularity of user interests and characterize the contribution of each pattern to the recommendation targets. However, properly modeling the conjunction interrelationships of items within union-level patterns and obtaining suitable representations pose challenges. The normal vector representation equipped with the dot product fails to learn such interrelationships [7], thereby leading to suboptimal results. Therefore, we turn to probabilistic embedding, which models each item as a collection of distributions. Recently, Gaussian embedding for uncertainty modeling [7] and Gamma/Beta embedding for logical reasoning (including the conjunction operation) have exhibited promising results [8], [9]. Within this context, the utilization of Gamma or Beta distributions is favored owing to their inherent closure property. This characteristic guarantees that the fused pattern representation remains within the identical probability space as the candidate item, thereby preserving the mathematical integrity of the model. Subsequently, the Kullback-Leibler (KL) divergence, as opposed to the Euclidean distance, is employed as a metric to assess the pattern contribution to candidate items. As such, a pattern is deemed to have a greater contribution on the recommendation

Kun Ma, Cong Xu, and Wei Zhang are with the School of Computer Science and Technology, East China Normal University, Shanghai, China. (email: 51255901097@stu.ecnu.edu.cn, congxueric@gmail.com, zhangwei.thu2011@gmail.com)

Zeyuan Chen is with the Ant Group, Hangzhou, China. (email: chen-zeyuan.czy@antgroup.com)

Manuscript received XX XX, 2023; revised XX XX, XXXX.

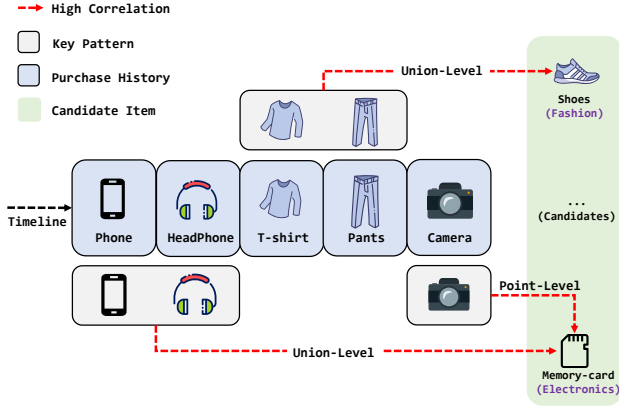


Fig. 1. Illustration of interpretability at the point-level and union-level. The former is commonly used in existing studies to identify key individual items, while the latter provides additional insights into the common interests exhibited by a user.

of a candidate item, if there is a reduced KL divergence observed between their respective distributions.

However, it is infeasible to directly conduct supervised training for automatically calculating the pattern contribution as the sequences are not labeled with key patterns. Minimizing the total distance to the positive samples while simultaneously maximizing the total distance to the negative samples is a feasible but problematic solution. In this vein, the optimization will skew towards non-critical patterns rather than key patterns due to the overwhelming number of non-critical patterns. To address this problem, we propose a correction method that combines a distance-based weight with a sequence-aware bias. The former assigns higher weights to current ‘key’ patterns, while the latter injects more user-specific information.

Our contributions can be summarized as follows:

- Previous sequence models have faced challenges in accurately identifying key items or have been limited to point-level interpretability. On the contrary, PTSR explicitly extracts fine-grained patterns allowing the estimation of both point-level and union-level pattern contributions.
- To accurately learn the interrelationships within union-level patterns, we employ probabilistic embedding instead of normal vector representation. This allows us to model the inherent uncertainties and dependencies in the data more effectively. Then, a pattern is considered to be more critical to the recommendation decision if its KL-Divergence to the recommended item is lower.
- Supervised pattern contribution learning is infeasible in practice due to the absence of labeled key patterns. A carefully designed pattern weighting correlation is developed to make it learnable.
- Extensive experiments have been conducted to demonstrate the superior recommendation performance of PTSR compared to eight baseline methods. Additionally, a case study further verifies the transparency of PTSR in providing explanations for its recommendation results.

TABLE I
NOTATIONS USED IN THIS PAPER

Notation	Description
s	user interaction sequence
v	item
l	level of pattern
$p_k^{(l)}$	the k -th pattern of the l -th level
α, β	parameters of the Gamma distribution
$f(\cdot; \alpha, \beta)$	probability density function(PDF)
η	distance-based weight
δ	sequence-aware bias
γ	margin parameter
$\mathbf{v} \in \mathbb{R}_{+}^{2d}$	item representation
$\mathbf{p} \in \mathbb{R}_{+}^{2d}$	pattern representation

II. RELATED WORK

A. Sequential Recommendation

Recommender systems are designed to retrieve items of interest to the user. Some early studies, such as general collaborative filtering [10], [11], adopt simple architectures, thereby achieving decent efficiency and a certain degree of interpretability (mostly point-level). Despite their satisfactory efficiency, the lack of sequential information confines them to static user profiles. Therefore, sequential models [12] are gaining increasing popularity within the research community due to their potential in dynamic interest modeling. The development of this field has closely followed the evolution of sequential modeling: embarking from traditional models [13], [14] based on Markov chains, to more recent techniques such as GRU4Rec [15], [16] and SASRec [4], where recurrent neural networks [17] and transformers [18] are employed, respectively. These sequential models, particularly attention-based approaches [4], [12], [5], have demonstrated impressive recommendation performance.

However, the increasing precision comes with rapidly deteriorating model transparency. Compared to general collaborative filtering, both the gated hidden unit utilized in GRU4Rec and the autoregressive attention mechanism employed in SASRec are more sophisticated yet lack interpretability. Consequently, they often fail to identify key items to support their predictions [6], [19], [20]. Although some efforts have been made to simplify the architectures (e.g., FMLP-Rec [21] is a pure MLP model), the decision transparency is inevitably compromised as more blocks are stacked to achieve sufficient model expressive power. In contrast, PTSR proposed in this paper is decision-transparent at the model architecture level while preserving satisfactory recommendation performance.

B. Explainable Recommendation

Compared to traditional recommendation models, explainable recommender systems enhance user trust by offering justifications for their recommendations, while maintaining high performance. In recent years, numerous significant studies have emerged in this field. These can be broadly categorized into two main groups based on their use of side information: similarity-based and aspect-based.

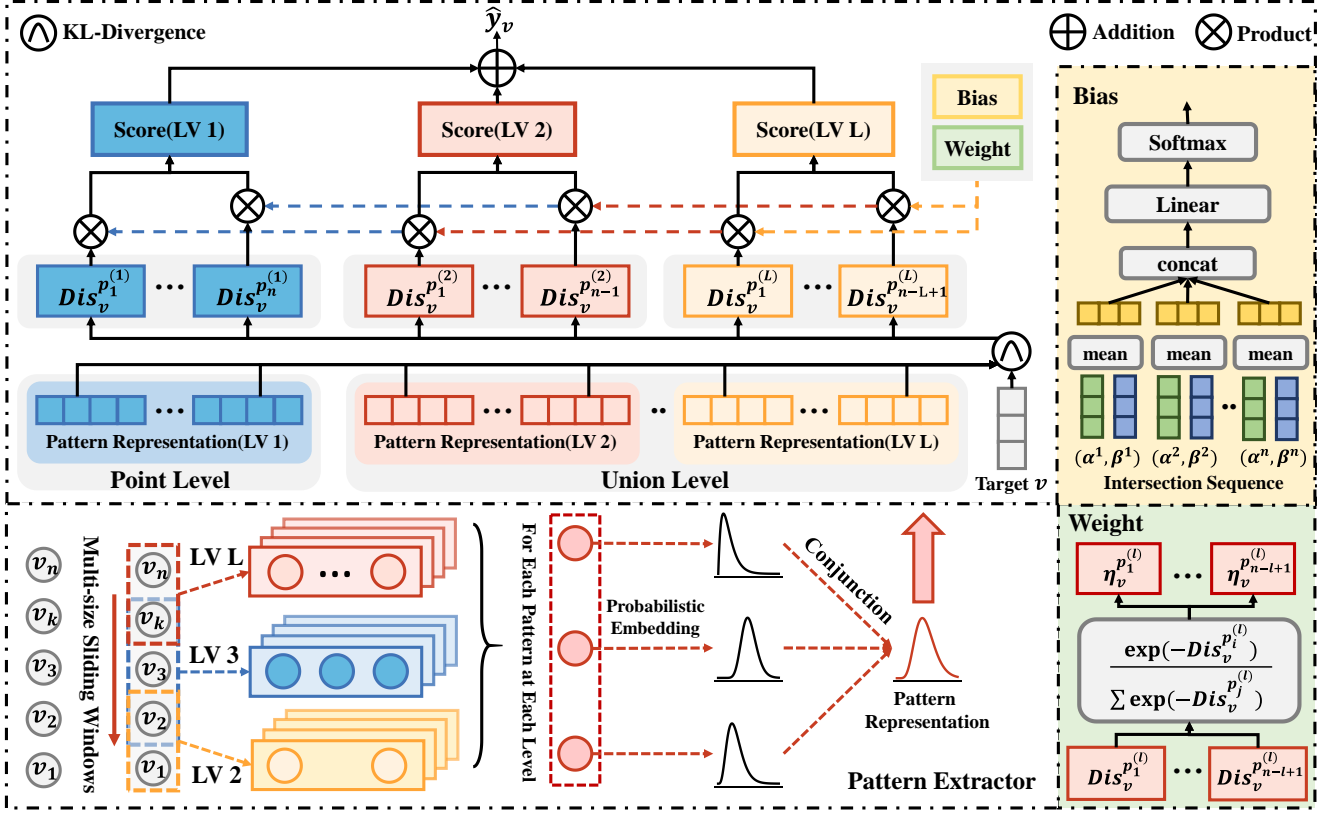


Fig. 2. Overview of PTSR.

Similarity-based models typically treat items holistically, modeling the relationships between them using transparent model structures without considering item-specific attribute associations. For example, Abdollahi et al. [22] introduces the use of Restricted Boltzmann Machines (RBM) to generate explainable top-N recommendation lists. Similarly, EMF [23] employs constrained matrix factorization for interpretable recommendations, mitigating the trade-off between interpretability and accuracy. NAIS [1] designs an attention network for interpretable collaborative filtering, which can identify significant items in the interaction sequence for prediction. RUM [2] develops user memory networks for sequential recommendation, extracting patterns to show how previous items affect future user actions. While these methods achieve both transparency and accuracy, they typically model only low-order item relationships to maintain transparent structure. In contrast, our method can transparently capture both low-order and high-order item relationships.

Aspect-based approaches, in contrast, often integrate external information (e.g., user reviews, item attributes, item relationships) to achieve fine-grained interpretability. EFM [24] analyzes user reviews to extract aspects of item and user perspectives, generating explanations through a matrix factorization-based model. TriRank [25] similarly analyzes item aspects from user reviews and models the user-item-aspect relationship using tripartite graphs, achieving explainable collaborative filtering. PGPR [26] constructs graphs using

item attributes and relational features, employing reinforcement learning to reason about target items, with the reasoning paths serving as explanations. NS-ICF [27] designs fully transparent three-tower structures based on neuro-rule networks [28], [29] for attribute-based recommendations based on neuro-symbolic methods, generating highly interpretable rules and corresponding weights. Counter [30] relies on counterfactual reasoning, where counterfactual explanations reveal which aspect changes affect item recommendations. These methods' explainability relies on rich and accurate aspect information; however, limited data may impact their effectiveness.

This work attempts to address the limitation of similarity-based methods in modeling higher-order item relationships by introducing probabilistic operators and only item ID is considered as input. It is beneficial for providing multi-level interpretability while achieving high accuracy.

C. Novel Embedding for Recommendation

Recently, novel types of embedding, such as distribution-based and geometry-based, etc., have begun to demonstrate remarkable performance. These embeddings differ fundamentally from traditional embedding by not confining users or items to a single point in vector space. Several studies have sought to integrate these advancements into recommendation systems to enhance model performance and cognitive capabilities. For instance, DDN [31], PMLAM [7], DT4SR [32], and

STOSA [33] have challenged the efficacy of the dot product, which is argued to violate the triangular inequality and lead to sub-optimal results. To address this, they propose modeling users and items as Gaussian distributions. Apart from those representations, other studies have explored Beta [8] and Gamma [34] distribution-based representations, introducing logical operators customized for closures that operate upon these distributions, thereby laying the groundwork for subsequent methodologies. For example, SRPLR [9] employs Beta embedding as foundational representations and merges its logical operators with neural networks to amplify the efficacy of traditional models. Beyond distribution types, geometry-based embedding gains popularity as well. Zhang et al. [35] propose the use of hypercuboids to explicitly represent and model user interests. CBox4CR [36] seeks to refine model cognition through Box embedding. This enables logical operations on their closures.

To harness the strong representational powers of these novel embeddings and the logical operators established upon them, we integrate probability distribution-based embeddings (e.g., Beta and Gamma embeddings) into our model, which facilitate capturing item relationships and modeling the pattern representations introduced later.

III. METHODOLOGY

In this section, we first briefly introduce the task of interpretable sequential recommendation, followed by details of Pattern-wise Transparent Sequential Recommendation (PTSR). In addition, the optimization objective of PTSR are succinctly clarified and the complexity of the model will be analyzed.

A. Problem Formulation

Given a user's historical interaction sequence $s = [v_1, v_2, \dots, v_n]$, where n is the maximum sequence length, sequential recommendation aims to predict the next item v_{n+1} that the user is most likely to click or purchase. Specifically, PTSR will score each candidate item to measure how well it matches the user's historical interactions. These scores then can be used to filter out the most relevant items from the candidates.

Apart from recommendation precision, there are additional requirements for an interpretable sequence model; that is, key items or item combinations belonging to the user interaction sequence s should be identified to account for the model's predictions. This poses a challenge to traditional approaches due to their black-box nature. In this paper, PTSR aims to identify a segment of the sequence (dubbed pattern) as the justification. The items within this pattern collectively explain why a high score is assigned to the recommended item.

B. Model Details of PTSR

Figure 2 illustrates the model architecture of PTSR including four modules:

1. **Multi-level Pattern Extraction.** Sliding windows of different sizes are first employed to extract fine-grained patterns

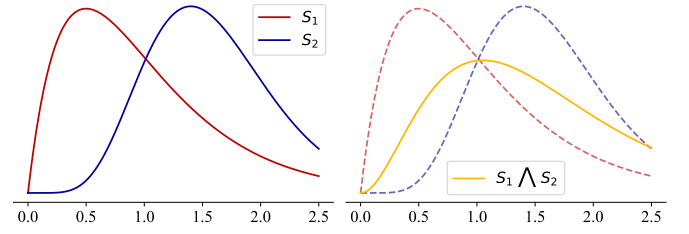


Fig. 3. Illustration of probabilistic conjunction operator. $S_1 \wedge S_2$ denotes the conjunction of distribution S_1 and S_2 , achieved by the weighted product of the probability density function (PDF).

by traversing the interaction sequence from left to right. Every pattern contains one or several consecutive item IDs.

2. **Pattern Representation Modeling.** For each pattern, PTSR transforms its item IDs into probabilistic embedding, and then conjoins the items using probabilistic conjunction [8], [34] to obtain the pattern representation.
3. **Pattern Contribution Estimation.** Firstly, the distance between each pattern representation and target item representation can be calculated by KL-Divergence. A weight unit then uses a softmax function to transform negative distance into non-normalized weights in conjunction with a sequence-aware bias. They are combined with distances to determine each pattern's contribution.

1) *Multi-level Pattern Extraction:* Previous methods primarily focus on the significance of low-order (point-level) item relationships to maintain decision transparency [2], [1]. Additionally, other approaches that account for higher-order (union-level) item relationships typically achieve this by stacking multiple neural network modules [4], [5], [33]. However, these higher-order relationships often lack interpretability due to the nonlinear functions involved in these modules. To model point-level and union-level item relationships while preserving model transparency, we begin by extracting multi-level patterns from the sequence directly, which form the **atomic units** for subsequent transparent decision-making process. To be more specific, it explicitly splits the sequence $s = [v_1, v_2, \dots, v_n]$ via a sliding window of size l , and the k -th segment is defined as follows:

$$p_k^{(l)} = [v_k, v_{k+1}, \dots, v_{k+l-1}], \quad k = 1, 2, \dots, n - l + 1.$$

Notably, patterns of different levels should be understood from different perspectives [37]:

- $p^{(1)}$ inherently is an individual item. Such *point-level* pattern appears simple but is capable of providing the most straightforward and human-friendly explanation. For example, the purchase of a camera rather than a T-shirt contributes more to the purchase of a memory card. A reliable sequence model should be able to accurately learn such similarities across items.
- Apart from the point-level pattern, a sliding window of size $l > 1$ yields *union-level* patterns, which consists of a group items interacted by the user sequentially. These union-level patterns are of great value in capturing the user intent at a deeper level. For example, the co-occurrence of 'phone' and 'headphone' implies a clear interest in electronics, also mak-

ing it reasonable to recommend ‘memory card’. This higher-order interpretability enhances clarity in understanding the combinational relationships between items. By mining the combinational display of multiple items based on users’ interactions, it becomes easier to gain users’ trust compared to relying on isolated single-item similarities.

Since both point-level and union-level patterns are essential for a transparent decision-making process, we collect all patterns with levels ranging from 1 to L . The remaining challenge lies in effectively integrating the items for pattern-wise representations.

2) *Pattern Representation Modeling*: It is straightforward to capture ‘common’ characteristics for point-level patterns but not so for union-level patterns. Previous methods of relative transparency typically embed each item into a learnable vector $\mathbf{v} \in \mathbb{R}^d$, and then the pattern representation is obtained in a weighted average manner:

$$\mathbf{p}_k = \sum_{i=k}^{k+l-1} w_i \cdot \mathbf{v}_i \in \mathbb{R}^d,$$

where w_i is the weight associated with \mathbf{v}_i (e.g., $w_i \equiv 1/l$ for mean pooling). However, this simple fusion of embeddings is still limited to similarity and cannot model complex relationships between items.

To address this issue, we resort to probabilistic embedding in the form of probability distributions (e.g., Gamma, Beta, and Gaussian). Specifically, the elements in \mathbf{v} consist of the parameters of probabilistic distribution. For example, the Gamma distribution is jointly described by a shape parameter $\alpha > 0$ and a scale parameter $\beta > 0$, while the Beta distribution is defined by two shape parameters (α, β) . Both of them yield the probabilistic embedding that resembles

$$\mathbf{v} = (\alpha, \beta) = [(\alpha_1, \beta_1), (\alpha_1, \beta_1), \dots, (\alpha_d, \beta_d)] \in \mathbb{R}_+^{2d}. \quad (1)$$

In this case, multiple independent distributions defined by different parameters can represent different characteristics of the item, which can enhance expressiveness [34], [8]. It has two distinct advantages over the normal vector representation: 1) The difference along the dimensions can be separately measured by probabilistic metrics such as Kullback-Leibler (KL) divergence instead of Euclidean distance. KL-Divergence can naturally model the asymmetry and uncertainty that prevail among items. 2) Complex relationships between items can be modelled using probabilistic operators (introduced next) based on probabilistic embeddings.

It is worth noting that other probability distributions with similar properties, such as the Gaussian distribution [38] or the Dirichlet distribution [39], are also applicable to our framework. However, due to space limitations, we will focus on the Gamma distribution [34] and the Beta distribution [8], which have a more uniform form for ease of elaboration. Denoted by $f(\cdot; \alpha, \beta)$ the probability density function (PDF), the product of a collection of PDFs can be derived as follows:

$$\prod_i f^{w_i}(\alpha_i, \beta_i) \propto f\left(\sum_i w_i \cdot \alpha_i, \sum_i w_i \cdot \beta_i\right). \quad (2)$$

This ‘weighted average’ operation is a scalar form of the probabilistic conjunction operation [8], which yields a PDF

measures how well the different distributions agree with each other. Probability distributions offer greater expressiveness than real values, allowing pattern representations obtained through probabilistic conjunction to capture complex interaction relationships between items more effectively than standard weighted fusion. We substantiate this claim with comparative experiments presented in Section IV-D.

We are now ready to extract the conjunction relationships within a single pattern. Given an l -length pattern $p_k = [v_k, v_{k+1}, \dots, v_{k+l-1}]$, a vectorized probabilistic conjunction then separately fuses items along the embedding dimension,

$$\mathbf{p}_k := \left(\sum_{i=k}^{k+l-1} \mathbf{w}_i \odot \alpha^{v_i}, \sum_{i=k}^{k+l-1} \mathbf{w}_i \odot \beta^{v_i} \right) \in \mathbb{R}_+^{2d}, \quad (3)$$

where \odot denotes the element-wise product, and a self-attentive mechanism is used to boost the model’s expressive power,

$$\mathbf{w}_i = \frac{\exp(\text{MLP}(\alpha^{v_i} \oplus \beta^{v_i}))}{\sum_{j=k}^{k+l-1} \exp(\text{MLP}(\alpha^{v_j} \oplus \beta^{v_j}))} \in \mathbb{R}^d,$$

where \oplus denotes the vector concatenation.

3) *Pattern Contribution Estimation*: For a given candidate item v , the most straightforward way to measure the relevance between pattern $p_k^{(l)}$ and v is to calculate the distance between their probabilistic embeddings using KL-Divergence. And the smaller the distance, the higher the correlation between $p_k^{(l)}$ and v . Specifically, it can be expressed as:

$$Dis_{v^{(l)}}^{p_k^{(l)}} = \sum_{i=1}^d \text{KL}(f(\alpha_i^{v_i}, \beta_i^v) \| f(\alpha_i^{p_k^{(l)}}, \beta_i^{p_k^{(l)}})) \quad (4)$$

Therefore, the primary principle of pattern contribution learning is to keep the key patterns close to the target item. However, due to the unavailability of ground-truth key patterns, supervised pattern contribution learning is infeasible in practice. One might expect that minimizing the sum of distances from the target item and simultaneously maximizing the distances from the negative item would produce satisfactory results, but it is not the case for some reasons below.

- The distance (i.e., the KL-Divergence) between key patterns and the target item may decrease rapidly at the beginning of training. Soon it becomes easier to reduce the distance of non-critical patterns, eventually leading to marginal contribution differences across various patterns.
- Summing the distances is too naïve to achieve competitive recommendation performance. Two different candidate items may be considered equally good in this vein despite the large difference in distance from the key pattern. For instance, consider a pattern p_1 whose distance to the candidate v_1 is 0.1 and to the candidate v_2 is 0.8. In contrast, another pattern p_2 has a distance of 4.9 to v_1 and 4.2 to v_2 . Compared to p_2 , p_1 is arguably the key pattern for both candidate items, and thus v_1 should be recommended as it receives more support from p_1 . But they are of the same value according to the summing distance.

Hence, it is necessary to correct the total distance for next-item recommendation in order to highlight the key patterns that have low distances from the target item.

Distance-based weight. Patterns deemed important will exhibit smaller distances from the target item and thus require larger weights to emphasize their contribution. Conversely, patterns far from the target item are of lower importance and should be assigned with smaller weights. For maintaining a proportional correspondence between the distance values and the weight values, the distance-based weights are normalized through a softmax function over the negative distances. For example, the weight of the k -th pattern at level l can be expressed as follows:

$$\eta_v^{p_k^{(l)}} = \frac{\exp(-Dis_v^{p_k^{(l)}})}{\sum_{j=1} \exp(-Dis_v^{p_j^{(l)}})}. \quad (5)$$

It is worth noting that the distance-based weights are independently calculated for each level. In this vein, patterns at the same level will compete with each other, and eventually, the most important patterns will stand out. Besides, patterns at different levels will collaborate to improve recommendation performance.

Sequence-aware bias. The distance-based weight can not only discern the importance of patterns but also detect alterations in the sequence of items, a crucial attribute in sequential recommendation. However, there is one exception to the incapacity to perceive changes in the sequence's order — when the entire sequence is reversed. The primary reason for this exception is that, in cases where only some items change their order, there must exist a pair of items that were not adjacent before but are now adjacent. In such instances, a sliding window of size 2 can capture this change. Nevertheless, when the entire sequence is reversed, there is no alteration in the adjacency between items.

We opt to introduce a sequence-aware bias to the distance-based weight, allowing it to adapt as the overall sequence order changes. Its practical significance lies in its interpretability as an evolutionary direction of user interest. Specifically, we employ an MLP to derive the sequence-aware weight, leveraging the sensitivity of the MLP to input order [40]. Concerning the input for the MLP, for each item in the sequence, we initially combine α and β in their Gamma embedding using $\frac{\alpha}{\alpha+\beta}$. The updated representation of the i -th item can be expressed as $\mathbf{e}_i = \frac{\alpha_i}{\alpha_i+\beta_i}$. This operation directly reduces the number of parameters in the MLP by half while preserving information compared to directly concatenating α and β . Subsequently, we concatenate these updated representations of all items to form the input for the MLP. For MLP's output, we also use softmax for normalization. The sequence-aware bias of k -th pattern at level l is expressed as follows:

$$\delta_k^{(l)} = [\text{Softmax}(\text{MLP}^{(l)}(\mathbf{e}_1 \oplus \dots \oplus \mathbf{e}_n))]_k, \quad (6)$$

where n is the sequence length. Since each level has a different number of patterns, we set the bias for each level individually.

Combining the distance-based weight and sequence-aware bias, we can get the final pattern correction weight $\eta_v^{p_k^{(l)}} + \lambda\delta_k^{(l)}$ where λ is a hyperparameter used to control the effect of bias.

TABLE II
DATASET STATISTICS AFTER PREPROCESSING.

Dataset	#Users	#Items	#Interactions	Avg. Len.	Sparsity
Beauty	22,363	12,101	198,502	8.87	99.93%
Toys	19,412	11,924	167,597	8.63	99.99%
Tools	16,638	10,217	134,476	8.08	99.92%
Yelp	30,431	20,033	316,354	10.39	99.95%

C. Prediction and Training Objective

With the pattern contribution, the eventually corrected score for prediction is defined as follows:

$$\hat{y}_v = \sum_{l=1}^L \cdot \left[\sum_{k=1}^{n-l+1} (\eta_v^{p_k^{(l)}} + \lambda\delta_k^{(l)}) \cdot (\gamma - Dis_v^{p_k^{(l)}}) \right]. \quad (7)$$

Note that \hat{y}_v differentially integrates contributions across patterns and levels. As a result, a high prediction score requires a strong agreement among the majority of key patterns, and thus key patterns can be implicitly learned even in the absence of ground-truth labels. In addition, γ is a margin hyperparameter to prevent \hat{y}_v from always being less than or equal to 0 during training.

The training objective of PTSR is the binary cross-entropy loss, which is designed to minimize the corrected score to target item v_+ , while simultaneously maximizing the corrected score to negative items v_- (uniformly sampling one negative sample for each positive item); that is,

$$\ell = -\log \sigma(\hat{y}_+) - \log \sigma(-\hat{y}_{v_-}). \quad (8)$$

D. Computational Complexity

For each pattern of length l , the complexity for the probabilistic conjunction operation is approximately $\mathcal{O}(ld^2)$. Since there are a total of $n - l + 1$ patterns per level, the main computational complexity of PTSR is $\mathcal{O}(nL^2d^2)$. Recall that a single self-attention module requires $\mathcal{O}(nd^2 + n^2d)$ overhead. Since $L = 2, 3$ is often the optimal value regardless of the performance (see Section IV-D) or interpretability point of view, the efficiency of PTSR therefore is comparable to that of normal attention-based methods.

IV. EXPERIMENTS

This section introduces extensive experiments to address the following five research questions:

- RQ1* How is the recommendation performance of PTSR compared to other sequence models?
- RQ2* To what extent do specific components (e.g., Weight, Bias) contribute to the effectiveness of PTSR?
- RQ3* What is the performance associated with varying levels of patterns?
- RQ4* How critical is the hyperparameter λ to the performance of PTSR?
- RQ5* How interpretable is PTSR in comparison to other methods?

A. Experimental Setup

Datasets. We evaluate our model on four publicly available datasets from two different sources:

- **Amazon** records user reviews of the site’s products. The data is divided into multiple datasets according to the category of items. We select **Beauty**, **Toys**, and **Tools** that are known for high data sparsity.
- **Yelp** is a famous merchant review website, by which the dataset released contains data on user ratings of merchants on the site.

Following [4], [41], we filter out the users and items with fewer than 5 interactions, and split the dataset in a *leave-one-out* fashion. The second last item is used for validation and the last item serves for testing. The statistics of the processed datasets have been summarized in Table II.

Evaluation metrics. We employ two commonly used metrics for model evaluation, including Normalized Discounted Cumulative Gain (NDCG) and Hit Ratio (HR). NDCG is a metric assessing the efficiency of a ranking system by considering the placement of relevant items within the ranked list. HR is the accuracy of ground-truth items that appear in top N recommendation list. To enhance the evaluation’s effectiveness, we employ *real-plus- N* [42] to calculate the metrics. More specifically, we randomly choose 100 items that users have not interacted with as negative samples. These are then combined with the ground truth to create a candidate set for ranking. NDCG@5, NDCG@10, HR@5, and HR@10 are reported.

B. Baselines

In order to fully demonstrate the effect of our model, we choose four different groups of recommendation baselines. The models in the first group utilize recurrent neural networks and classical convolution operations to model user interests:

- **GRU4Rec** [15]: Early proposal of using GRU to model user action sequences, mainly applied to session-based recommendation.
- **Caser** [37]: A method that treats user behavior sequences as ‘image’ and use convolution kernels to learn sequential patterns.

The next two models serve as the interpretable baselines:

- **NAIS** [1]: Through a more transparent attention network, it is capable of distinguishing which historical items in a user profile are more important for a prediction.
- **RUM** [2]: It introduces a memory mechanism to dynamically manage user interaction records and capture the importance of items in the interaction history.

The methods in the third group leverage the self-attention mechanism to model long-term behavioral patterns:

- **SASRec** [4]: A classic model in sequential recommendation, applying a left-to-right attention mask to capture user’s behavior.
- **BERT4Rec** [5]: A method using a bidirectional self-attention mechanism, introducing a cloze task to predict masked items.

The fourth group of baselines applies novel embedding (such as probabilistic embedding, box embedding) to recommendation task, which improves the modeling and representation capabilities:

- **STOSA** [33]: This approach involves embedding items as stochastic Gaussian distributions and introducing a novel Wasserstein Self-Attention module to characterize item-item relationships.
- **CBox4CR** [36]: It uses box embedding to represent items, so it can model user and item in a closed manner and introduce logical operators based on box embedding.
- **SRPLR** [9]: It is a relatively novel framework that combines deep learning with symbolic learning, which utilizes Beta embedding to model logical relationships. We set its backbone to SASRec.

Implementation details. We implement PTSR using PyTorch and employ the Adam optimizer [43] with a learning rate of 0.0005, and a weight decay coefficient searched within $\{1e-9, 1e-8, 1e-7, 1e-6\}$. Regarding the number of pattern levels, we set it to 3 for Yelp dataset and 2 for the other three. The margin γ in Equation 7 is set to 2. Following previous studies [9], [36], the embedding size of either α or β is fixed to 64. The hyper-parameter λ for enhancing the sequence-aware bias is discussed in Section IV-F.

We reproduce the results of CBox4CR, STOSA, and SRPLR according to their official code, and the implementation for other models mainly due to RecBole [44]. We employ a grid search strategy to meticulously explore optimal hyper-parameters for all baselines. For fair comparisons, only implicit feedback interactions are available for all methods during training. The maximum sequence length is set to 20 as the average sequence length is around 10 for all the datasets. All the methods are trained from scratch on a single NVIDIA GeForce RTX 2080 Ti GPU with a batch size of 512.

C. Recommendation Performance Comparison (RQ1)

We compare PTSR with other sequence models to validate the superiority in achieving state-of-the-art recommendation performance. The experimental results have been presented in Table III, from which we can draw three key conclusions:

- Traditional sequence models, especially Transformer-based approaches such as SASRec and BERT4Rec, are already capable of achieving satisfactory recommendation performance. By applying novel (distribution-based and geometry-based) embeddings, STOSA, CBox4CR, and SPRLR have demonstrated further performance improvements. However, the black-box nature of these models hinders users from understanding their decision-making process, thus affecting the customer experience.
- NAIS and RUM are two alternatives able to provide point-level analysis to justify an individual item’s contribution to their recommendation results. However, it is clear that their interpretability comes at a huge cost in terms of performance, which is nearly 17.6% worse compared to state-of-the-art sequential approaches. In contrast, PTSR with Gamma embedding strikes a good balance between

TABLE III

OVERALL PERFORMANCE COMPARISON ACROSS FOUR DATASETS. THE BEST RESULTS AMONG ALL METHODS ARE MARKED IN **BOLD**, WHILE THE BEST RESULTS AMONG THE BASELINES ARE UNDERLINED. ‘IMPROV.’ REPRESENTS THE RELATIVE IMPROVEMENT OVER THE BEST BASELINE. PAIRED T-TEST IS PERFORMED OVER 5 INDEPENDENT RUNS FOR EVALUATING p -VALUE (* INDICATES STATISTICAL SIGNIFICANCE WITH A p -VALUE < 0.01). PTSR-B/G INDICATES THE USE OF BETA/GAMMA EMBEDDING.

Dataset	Metric	Traditional		Transparent		Attention-Based		Novel Embedding			Ours			
		Caser	GRU4Rec	NAIS	RUM	SASRec	BERT4Rec	STOSA	CBox4CR	SRPLR	PTSR-B	Improv.	PTSR-G	Improv.
Beauty	HR@5	0.3206	0.3402	0.3256	0.3763	0.3882	0.3989	0.3725	0.3997	<u>0.4100</u>	0.4491*	9.54%	0.4512*	10.05%
	HR@10	0.4252	0.4410	0.4240	0.4764	0.4832	0.4987	0.4772	<u>0.5044</u>	0.5024	0.5532*	9.67%	0.5573*	10.49%
	NDCG@5	0.2303	0.2511	0.2379	0.2779	0.2963	0.3039	0.2737	0.2959	<u>0.3219</u>	0.3395*	5.47%	0.3404*	5.75%
	NDCG@10	0.2641	0.2836	0.2696	0.3102	0.3270	0.3361	0.3075	0.3297	<u>0.3517</u>	0.3731*	6.08%	0.3747*	6.54%
Toys	HR@5	0.3014	0.3308	0.2935	0.3420	0.3867	0.3734	0.3816	0.3791	<u>0.4076</u>	0.4291*	5.27%	0.4302*	5.54%
	HR@10	0.4009	0.4367	0.3876	0.4409	0.4925	0.4786	0.4795	0.4848	<u>0.5035</u>	0.5344*	6.14%	0.5347*	6.20%
	NDCG@5	0.2179	0.2392	0.2161	0.2533	0.2866	0.2799	0.2898	0.2775	<u>0.3186</u>	0.3256*	2.20%	0.3276*	2.82%
	NDCG@10	0.2500	0.2734	0.2464	0.2853	0.3208	0.3139	0.3213	0.3116	<u>0.3495</u>	0.3597*	2.92%	0.3614*	3.40%
Tools	HR@5	0.2188	0.2350	0.2349	0.2618	0.2891	<u>0.3017</u>	0.2905	0.2758	0.2836	0.3425*	13.52%	0.3377*	11.93%
	HR@10	0.3135	0.3414	0.3266	0.3632	0.3885	<u>0.4067</u>	0.3897	0.3832	0.3813	0.4534*	11.48%	0.4485*	10.28%
	NDCG@5	0.1520	0.1618	0.1679	0.1863	0.2107	<u>0.2185</u>	0.2120	0.1943	0.2094	0.2495*	14.19%	0.2458*	12.49%
	NDCG@10	0.1824	0.1961	0.1974	0.2190	0.2427	<u>0.2523</u>	0.2440	0.2289	0.2408	0.2853*	13.08%	0.2815*	11.57%
Yelp	HR@5	0.5357	0.5661	0.5275	0.6075	0.5986	0.6167	0.5695	<u>0.6383</u>	0.6247	0.6677*	4.61%	0.6651*	4.20%
	HR@10	0.6988	0.7322	0.7023	0.7660	0.7639	0.7599	0.7329	<u>0.8026</u>	0.7797	0.8138*	1.40%	0.8107*	1.01%
	NDCG@5	0.3772	0.3998	0.3711	0.4459	0.4339	0.4567	0.4117	<u>0.4622</u>	0.4609	0.5013*	8.46%	0.5025*	8.72%
	NDCG@10	0.4301	0.4537	0.4277	0.4973	0.4875	0.5032	0.4646	<u>0.5156</u>	0.5113	0.5487*	6.42%	0.5498*	6.63%

TABLE IV

ABLATION STUDY(NDCG@5, NDCG@10, HR@5, HR@10) ON FOUR DATASETS, WITH BEST EFFECTS HIGHLIGHTED IN BOLD.

Architecture	Beauty				Toys				Tools				Yelp			
	N@5	N@10	HR@5	HR@10	N@5	N@10	HR@5	HR@10	N@5	N@10	HR@5	HR@10	N@5	N@10	HR@5	HR@10
Default	0.3404	0.3747	0.4512	0.5573	0.3276	0.3614	0.4302	0.5347	0.2458	0.2815	0.3377	0.4485	0.5025	0.5498	0.6651	0.8107
w/o W	0.3007	0.3337	0.4008	0.5030	0.2968	0.3306	0.3918	0.4963	0.1718	0.2089	0.2537	0.3687	0.4155	0.4725	0.5888	0.7644
w/o B	0.3228	0.3593	0.4376	0.5502	0.2980	0.3355	0.4040	0.5199	0.2398	0.2754	0.3357	0.4456	0.4979	0.5454	0.6632	0.8094
w/o W + B	0.2490	0.2832	0.3428	0.4489	0.2204	0.2548	0.3093	0.4163	0.1672	0.2003	0.2399	0.3428	0.4131	0.4646	0.5664	0.7257
Replace KL	0.2397	0.2720	0.3317	0.4317	0.1879	0.2208	0.2620	0.3640	0.1845	0.2165	0.2592	0.3588	0.3423	0.4029	0.4911	0.6784
Replace ProbE	0.2163	0.2533	0.3106	0.4247	0.1908	0.2294	0.2697	0.3896	0.1737	0.2077	0.2502	0.3556	0.3398	0.3973	0.4808	0.6592

performance and interpretability. It achieves better recommendation performance on the four datasets, with an average improvement of 5.23%.

D. Ablation Study (RQ2)

The results of the ablation experiments are presented in Table IV, which is divided into two main parts. The first part examines the effect of removing certain components on PTSR, while the second part investigates the impact of combining different positional encodings with PTSR. In the following, we describe the meaning of each part and analyze its effects:

- *w/o W (Weight)*: After calculating the distance between the pattern and the candidate item, we convert the negative distance into a weight using a softmax function within the weight unit. This weight is then multiplied by the distance to determine the pattern’s contribution. If the weight unit is removed, the distance itself is directly used as the pattern’s contribution. Compared to *DEFAULT*, this variant is significantly less effective. The primary reason for this is that without the weights, the distances of both the key

and noise patterns converge around the margin, leading to lower differentiation. Adding the weight units emphasizes the decisive role of the key pattern in scoring by assigning it a larger weight.

- *w/o B (Bias)*: We utilize sequence-aware bias to enhance PTSR’s ability to capture sequential information. As illustrated in Table IV, the removal of this bias significantly affects the Beauty and Toys datasets, while its impact on the Tools and Yelp datasets is relatively minor, underscoring the critical role of this component for PTSR. Notably, our model is capable of capturing certain sequential information even without sequence-aware bias. For instance, altering the sequence $[a, b, c]$ to $[a, c, b]$ results in distinct patterns $\{\{a, b\}, \{b, c\}\}$ and $\{\{a, c\}, \{c, b\}\}$ with a window of size 2. Conversely, reversing the sequence to $[c, b, a]$ yields the same patterns as $[a, b, c]$. In such cases, bias further enhances the model’s ability to perceive sequence changes. Therefore the order information is derived from both sequence-aware bias and inherent patterns, and a smaller influence of bias may suggest that the pattern itself

TABLE V
PERFORMANCE OF SINGLE-LEVEL AND MULTI-LEVEL ON FOUR DATASETS.

Level of Pattern		Beauty				Toys				Tools				Yelp			
		N@5	N@10	HR@5	HR@10	N@5	N@10	HR@5	HR@10	N@5	N@10	HR@5	HR@10	N@5	N@10	HR@5	HR@10
Single-level	1	0.3268	0.3621	0.4372	0.5462	0.3085	0.3434	0.4103	0.5185	0.2215	0.2579	0.3125	0.4252	0.4668	0.5184	0.6408	0.7997
	2	0.3140	0.3492	0.4259	0.5350	0.3020	0.3387	0.4066	0.5205	0.2253	0.2626	0.3173	0.4327	0.4534	0.5063	0.6302	0.7927
	3	0.3056	0.3405	0.4159	0.5235	0.2942	0.3312	0.4019	0.5161	0.2237	0.2604	0.3161	0.4299	0.4464	0.5006	0.6210	0.7877
Multi-level	{1}	0.3268	0.3621	0.4372	0.5462	0.3085	0.3434	0.4103	0.5185	0.2215	0.2579	0.3125	0.4252	0.4668	0.5184	0.6408	0.7997
	{1,2}	0.3404	0.3747	0.4512	0.5573	0.3276	0.3614	0.4302	0.5347	0.2458	0.2815	0.3377	0.4485	0.5004	0.5482	0.6665	0.8135
	{1,2,3}	0.3367	0.3701	0.4425	0.5454	0.3251	0.3571	0.4276	0.5266	0.2409	0.2749	0.3252	0.4309	0.5025	0.5498	0.6651	0.8107

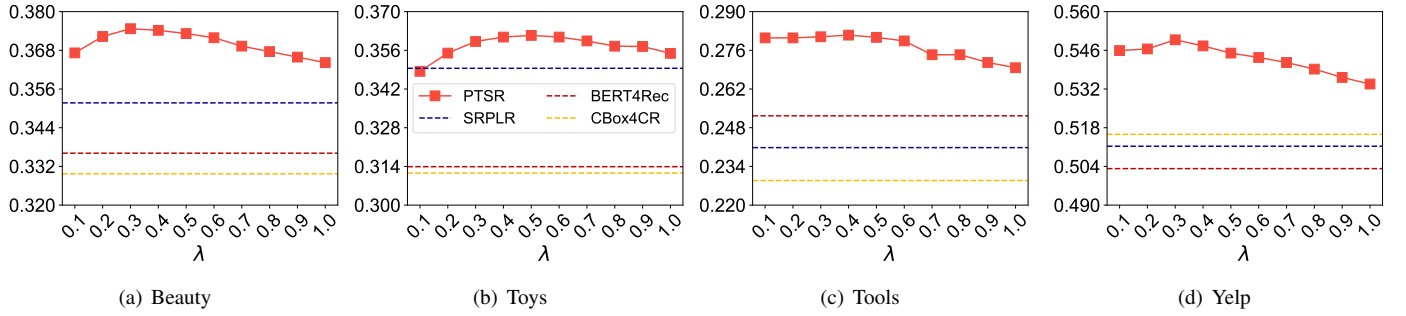


Fig. 4. NDCG@10 performance over various λ on four datasets.

plays a predominant role.

- *w/o W+B (Weight and Bias)*: When both weight and bias are removed, PTSR derives the score of the candidate item solely by aggregating the distances of patterns, relying on the intrinsic characteristics of the patterns to perceive sequence information. This approach is the most fundamental structure without any auxiliary mechanisms to aid optimization. Unsurprisingly, this results in a significant performance decline of 15% to 30%, unequivocally demonstrating the crucial combined impact of weight and bias on the efficacy of PTSR.
- *Replace KL (KL-Divergence)*: Since PTSR is based on Beta/Gamma embedding, we employ KL-Divergence to calculate the distance between the distribution of the pattern and that of the target item. To investigate the impact of KL-Divergence, we replace it with cosine similarity as the metric. Table IV demonstrates a substantial decrease in PTSR's effectiveness. We attribute this decline to several factors: (1) the value range of cosine similarity is $[0, 1]$, whereas KL-Divergence spans $(0, +\infty)$, allowing KL-Divergence to better capture differences; (2) KL-Divergence is more adept at measuring distributional discrepancies; and (3) KL-Divergence is asymmetric, which is particularly suitable for recommendation scenarios. For example, the probability of purchasing a computer followed by a desk differs from the probability of purchasing a desk followed by a computer, a distinction that KL-Divergence can effectively capture.
- *Replace ProbE (Probabilistic Embedding)*: To explore the impact of embedding, we substitute probabilistic embedding with ordinary embedding. Specifically, we replace the

probabilistic conjunction operator unique to probabilistic embedding with an ordinary weighted sum. Except for the Toys dataset, the experimental results show an even greater decrease in performance compared to the replacement with KL-Divergence. Thus, we argue that the efficacy of PTSR primarily stems from the sophistication of probabilistic embedding, which offers interpretable probabilistic operators. Additionally, KL-Divergence further enhances the advantages of probabilistic embedding, making PTSR significantly more effective than the baselines.

E. Analysis of Pattern Level (RQ3)

In Section III, we elucidate the roles of point-level and union-level. In this section, we will delve into a thorough examination of the performance of single-level and multi-level. It should be noted that 'point-level' and 'union-level' refer to the granularity of items, with 'point' denoting a single item and 'union' indicating a combination of items. Similarly, 'single-level' and 'multi-level' refer to the granularity of levels, where 'single' denotes a single level and 'multi' signifies a combination of levels.

As shown in Table V, we conduct two sets of experiments. The first set is single-level, where we use a single sliding window to extract patterns from a specific level. The second set is multi-level, where $\{1,2,3\}$ means that we simultaneously use window sizes of 1, 2, and 3 for extraction. The results reveal two observations:

- When only using one level of patterns (i.e., single-level), high levels do not exhibit the same performance as low levels. This phenomenon indicates low levels, especially point-level, play a foundation role in sequential recommendation.

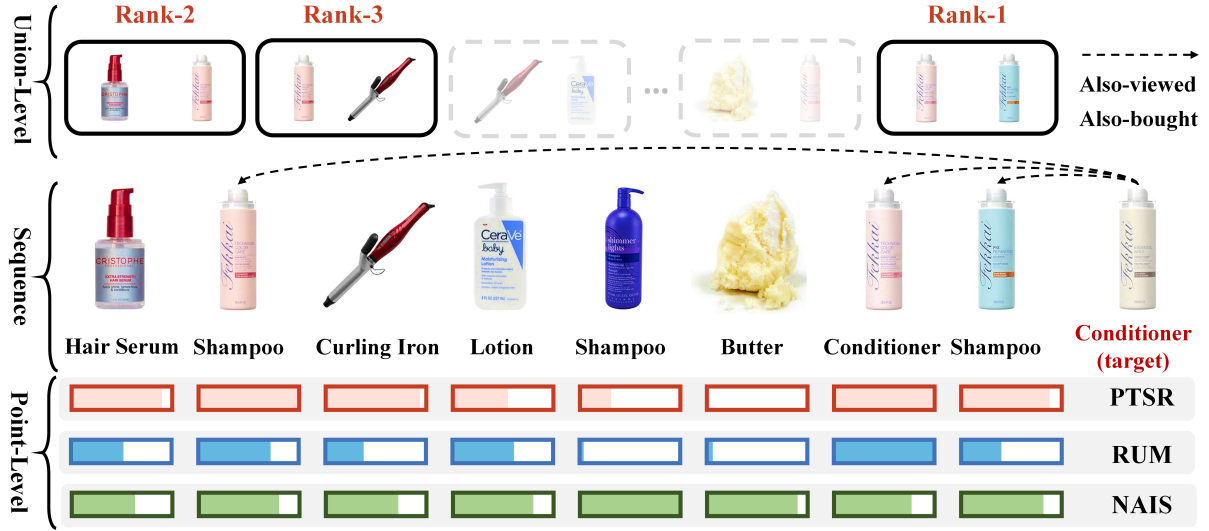


Fig. 5. A case study of a real user. ‘Point-level’ compares the interpretability of an individual item’s contribution to the target, while ‘Union-level’ selects a group key items account for recommendation.

- When using multiple levels of patterns, the recommendation performance could be improved. Specifically, the best result is achieved with the combinations 1, 2 for Beauty, Toys, and Tools datasets, and 1, 2, 3 for the Yelp dataset. This is attributed to the effectiveness of integrating different levels, as each captures user interests at varying granularities and offers distinct interpretability.

F. Impact of Hyperparameter λ (RQ4)

We investigate the sensitivity of the hyperparameter λ introduced for controlling the effect of sequence-aware bias. We evaluate it on four datasets with values ranging from 0 to 1. As illustrated in Figure 4, for most datasets (Beauty, Toys, and Yelp), the performance initially increases and reaches its peak at approximately $\lambda = 0.4$. However, further increasing this value deteriorates the performance as the distance-based weight becomes overly weakened. Despite this, PTSR with $\lambda \approx 1$ consistently outperforms other recommendation methods (SRPLR, BERT4Rec, and CBox4CR), reaffirming the superiority of PTSR. An exception is the Tools dataset, in which the explicit sequence-aware bias has a negligible effect. We hypothesize that the pattern extraction process itself retains sufficient sequence information, which appears to be adequate for the Tools dataset.

G. Interpretability Analysis (RQ5)

In this section, we assess the interpretability of PTSR using the Beauty dataset. Following [45], [46], items that have a ‘Also-viewed’, ‘Also-bought’ or ‘Bought-together’, relationship with the target item are considered important. Therefore, the desired model should assign a high correlation/contribution value to these key items. In addition to a case study of a real-world user, we also give statistical results for the reliability of the assessment [47].

Case Analysis. Figure 5 first shows a real user’s interaction sequence, and the recommenders need to justify why the next

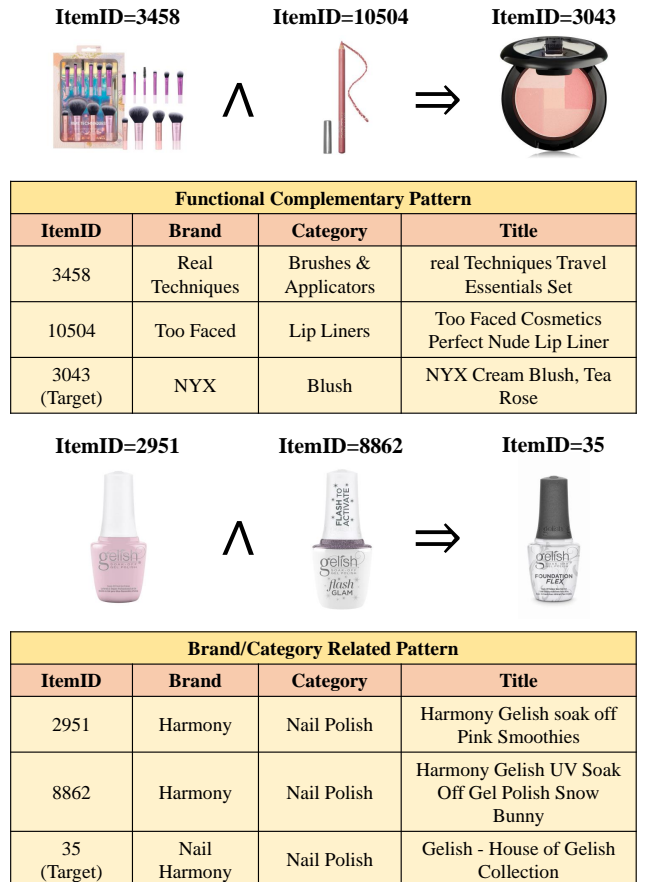


Fig. 6. Showcase of different types of union-level patterns.

item the user buys is ‘Conditioner’. In this case, only PTSR correctly highlights all interacted items with ‘Also Bought’ and ‘Also Viewed’ relationships. It is easy to see from the thumbnails that these key items belong to the same brand as

TABLE VI

KEY ITEMS RECALL (RECALL@1,2,3,5) ACROSS THREE AMAZON DATASETS. GIVEN A TARGET ITEM, THE MODEL NEEDS TO RETRIEVE AS MANY KEY ITEMS AS POSSIBLE FROM THE INTERACTION SEQUENCE WITH SPECIFIC RELATIONSHIPS, INCLUDING ‘ALSO-VIEWED’, ‘ALSO-BOUGHT’, AND ‘BOUGHT-TOGETHER’.

		Beauty				Toys				Tools			
Relationship	Method	R@1	R@2	R@3	R@5	R@1	R@2	R@3	R@5	R@1	R@2	R@3	R@5
Also-viewed	PTSR	54.72	67.26	76.83	87.81	68.72	75.63	82.24	91.46	52.11	65.25	74.88	87.21
	RUM	37.25	46.99	55.79	73.75	50.45	55.32	61.94	79.80	36.42	44.75	54.71	75.41
	NAIS	19.15	29.54	42.43	66.93	24.21	35.44	49.46	75.73	34.61	45.08	58.02	77.54
Also-bought	PTSR	56.08	68.3	78.42	89.63	70.13	76.51	82.96	92.07	66.67	74.65	82.37	92.73
	RUM	38.54	48.24	57.57	75.94	51.32	56.06	62.87	80.59	41.89	49.22	58.31	78.65
	NAIS	21.59	31.76	44.55	69.03	26.39	37.41	51.52	77.22	40.35	50.66	63.13	83.07
Bought-together	PTSR	53.41	71.46	83.12	94.1	64.16	76.31	86.66	95.82	69.67	82.04	90.06	96.85
	RUM	32.63	44.88	54.37	73.83	45.13	50.81	60.68	82.43	42.89	51.67	61.98	82.43
	NAIS	10.88	19.32	33.90	65.56	12.50	24.93	41.69	76.78	44.87	57.12	71.63	89.02

the target item. Instead, because NAIS consistently assigns high contributions to all items, it is impossible to distinguish them from one another. While RUM performs relatively well, it still lags behind PTSR in two aspects: 1) The most recent item (shampoo) receives a lower weight in RUM’s contribution estimation, which somewhat contradicts the common sense that the item with which the user has most recently interacted is usually more responsive to current interests. 2) PTSR can provide interpretability beyond the point level. Figure 6 illustrates the various types of patterns captured by PTSR in real-world scenarios. Remarkably, even without providing any information beyond the item ID, PTSR can still identify meaningful combinations of items through logical modeling.

Statistical Analysis. We further provide a statistical analysis to evaluate the interpretability in a comprehensive manner. Given a sequence and its subsequent target item, we can 1) identify the contribution of each item within the sequence to the target through the aforementioned interpretable models and 2) infer the ground-truth key items for the target according to specific relationships (‘Also-viewed’, ‘Also-bought’, and ‘Bought-together’). Hence, when those key items within a sequence are accurately associated with higher contribution, the model can be considered to possess better interpretability. Formally, the key items recalled over the dataset can be used to quantitatively evaluate the interpretability of models.

Table VI reports the comparisons. Both PTSR and RUM demonstrate competitive results, with items closely related to the target generally being ranked higher. It is worth noting that PTSR significantly outperforms RUM when only considering the top-ranked item (e.g., R@1), as the items that PTSR identifies as important are typically more reliable than those suggested by RUM. The overall performance of NAIS is not satisfactory, as it appears to assign less importance to key items.

V. CONCLUSIONS AND FUTURE WORK

In this work, we design a probabilistic embedding-based transparent network for interpretable sequential recommendation. Our primary motivation is that items in an interaction sequence influence the recommendation of the next item, either individually (low-order, point-level) or in combination

(high-order, union-level). We therefore propose using sliding windows to extract multi-level patterns and employing a probabilistic embedding-based conjunction operator to model high-order patterns, ensuring complete transparency of PTSR. Weight module is designed to highlight the different importance of patterns and aid optimisation. Sequence-aware bias aims to help the model perceive sequential information. Experimental results demonstrate PTSR is not only highly transparent and interpretable but also significantly outperforms classic sequential recommendation models w.r.t. recommendation performance.

Despite the promising results achieved by PTSR, several limitations remain. For instance, PTSR currently captures higher-order patterns based on neighboring items, but it fails to identify relationships among items that are spaced apart. Accurately detecting higher-order patterns corresponding to strongly correlated yet scattered items across multiple positions is challenging, as it requires maintaining the transparency of the process. Fortunately, recent advances in neural symbolic learning, [48], [49] which can automatically learn logical rules from discrete inputs, offer a potential solution. Therefore, in future work, we aim to explore models that can automatically search for items to form higher-order patterns, thereby enhancing the model’s flexibility. Additionally, our current approach employs only the conjunction operator, so we are also interested in integrating more logical operators into PTSR to improve its logical reasoning capability.

REFERENCES

- [1] X. He, Z. He, J. Song, Z. Liu, Y. Jiang, and T. Chua, “NAIS: neural attentive item similarity model for recommendation,” *IEEE Trans. Knowl. Data Eng.*, vol. 30, no. 12, pp. 2354–2366, 2018.
- [2] X. Chen, H. Xu, Y. Zhang, J. Tang, Y. Cao, Z. Qin, and H. Zha, “Sequential recommendation with user memory networks,” in *WSDM*, 2018, pp. 108–116.
- [3] Y. Zhang and X. Chen, “Explainable recommendation: A survey and new perspectives,” *Found. Trends Inf. Retr.*, pp. 1–101, 2020.
- [4] W. Kang and J. J. McAuley, “Self-attentive sequential recommendation,” in *ICDM*, 2018, pp. 197–206.
- [5] F. Sun, J. Liu, J. Wu, C. Pei, X. Lin, W. Ou, and P. Jiang, “Bert4rec: Sequential recommendation with bidirectional encoder representations from transformer,” in *CIKM*, 2019, pp. 1441–1450.
- [6] S. Serrano and N. A. Smith, “Is attention interpretable?” in *ACL*, 2019, pp. 2931–2951.

- [7] C. Ma, L. Ma, Y. Zhang, R. Tang, X. Liu, and M. Coates, “Probabilistic metric learning with adaptive margin for top-k recommendation,” in *KDD*, 2020, pp. 1036–1044.
- [8] H. Ren and J. Leskovec, “Beta embeddings for multi-hop logical reasoning in knowledge graphs,” in *NeurIPS*, 2020.
- [9] H. Yuan, P. Zhao, X. Xian, G. Liu, Y. Liu, V. S. Sheng, and L. Zhao, “Sequential recommendation with probabilistic logical reasoning,” in *IJCAI*, 2023, pp. 2432–2440.
- [10] X. He, L. Liao, H. Zhang, L. Nie, X. Hu, and T. Chua, “Neural collaborative filtering,” in *WWW*, 2017, pp. 173–182.
- [11] Y. Koren, “Collaborative filtering with temporal dynamics,” in *KDD*, 2009, pp. 447–456.
- [12] J. Li, Y. Wang, and J. J. McAuley, “Time interval aware self-attention for sequential recommendation,” in *WSDM*, 2020, pp. 322–330.
- [13] S. Rendle, C. Freudenthaler, and L. Schmidt-Thieme, “Factorizing personalized markov chains for next-basket recommendation,” in *WWW*, 2010, pp. 811–820.
- [14] R. He and J. J. McAuley, “Fusing similarity models with markov chains for sparse sequential recommendation,” in *ICDM*, 2016, pp. 191–200.
- [15] B. Hidasi, A. Karatzoglou, L. Baltrunas, and D. Tikk, “Session-based recommendations with recurrent neural networks,” in *ICLR*, 2016.
- [16] B. Hidasi and A. Karatzoglou, “Recurrent neural networks with top-k gains for session-based recommendations,” in *CIKM*, 2018, pp. 843–852.
- [17] K. Cho, B. van Merriënboer, D. Bahdanau, and Y. Bengio, “On the properties of neural machine translation: Encoder-decoder approaches,” in *SSST@EMNLP*, 2014, pp. 103–111.
- [18] A. Vaswani, N. Shazeer, N. Parmar, J. Uszkoreit, L. Jones, A. N. Gomez, L. Kaiser, and I. Polosukhin, “Attention is all you need,” in *NIPS*, 2017, pp. 5998–6008.
- [19] S. Jain and B. C. Wallace, “Attention is not explanation,” in *NAACL-HLT*, 2019, pp. 3543–3556.
- [20] S. Wiegreffe and Y. Pinter, “Attention is not not explanation,” in *EMNLP-IJCNLP*, 2019, pp. 11–20.
- [21] K. Zhou, H. Yu, W. X. Zhao, and J. Wen, “Filter-enhanced MLP is all you need for sequential recommendation,” in *WWW*, 2022, pp. 2388–2399.
- [22] B. Abdollahi and O. Nasraoui, “Explainable restricted boltzmann machines for collaborative filtering,” in *ICML*, 2016.
- [23] —, “Using explainability for constrained matrix factorization,” in *RecSys*, 2017, pp. 79–83.
- [24] Y. Zhang, G. Lai, M. Zhang, Y. Zhang, Y. Liu, and S. Ma, “Explicit factor models for explainable recommendation based on phrase-level sentiment analysis,” in *SIGIR*, 2014, pp. 83–92.
- [25] X. He, T. Chen, M. Kan, and X. Chen, “Trirank: Review-aware explainable recommendation by modeling aspects,” in *CIKM*, 2015, pp. 1661–1670.
- [26] Y. Xian, Z. Fu, S. Muthukrishnan, G. de Melo, and Y. Zhang, “Reinforcement knowledge graph reasoning for explainable recommendation,” in *SIGIR*, 2019, pp. 285–294.
- [27] W. Zhang, J. Yan, Z. Wang, and J. Wang, “Neuro-symbolic interpretable collaborative filtering for attribute-based recommendation,” in *WWW*, 2022, pp. 3229–3238.
- [28] Z. Wang, W. Zhang, N. Liu, and J. Wang, “Learning interpretable rules for scalable data representation and classification,” *IEEE Trans. Pattern Anal. Mach. Intell.*, vol. 46, no. 2, pp. 1121–1133, 2024.
- [29] W. Zhang, Y. Liu, Z. Wang, and J. Wang, “Learning to binarize continuous features for neuro-rule networks,” in *IJCAI*, 2023, pp. 4584–4592.
- [30] J. Tan, S. Xu, Y. Ge, Y. Li, X. Chen, and Y. Zhang, “Counterfactual explainable recommendation,” in *CIKM*, 2021, pp. 1784–1793.
- [31] L. Zheng, C. Li, C. Lu, J. Zhang, and P. S. Yu, “Deep distribution network: Addressing the data sparsity issue for top-n recommendation,” in *SIGIR*, 2019, pp. 1081–1084.
- [32] Z. Fan, Z. Liu, S. Wang, L. Zheng, and P. S. Yu, “Modeling sequences as distributions with uncertainty for sequential recommendation,” in *CIKM*, 2021, pp. 3019–3023.
- [33] Z. Fan, Z. Liu, Y. Wang, A. Wang, Z. Nazari, L. Zheng, H. Peng, and P. S. Yu, “Sequential recommendation via stochastic self-attention,” in *WWW*, 2022, pp. 2036–2047.
- [34] D. Yang, P. Qing, Y. Li, H. Lu, and X. Lin, “Gammae: Gamma embeddings for logical queries on knowledge graphs,” in *EMNLP*, 2022, pp. 745–760.
- [35] S. Zhang, H. Liu, A. Zhang, Y. Hu, C. Zhang, Y. Li, T. Zhu, S. He, and W. Ou, “Learning user representations with hypercuboids for recommender systems,” in *WSDM*, 2021, pp. 716–724.
- [36] T. Liang, Y. Zhang, Q. Di, C. Xia, Y. Li, and Y. Yin, “Contrastive box embedding for collaborative reasoning,” in *SIGIR*, 2023, pp. 38–47.
- [37] J. Tang and K. Wang, “Personalized top-n sequential recommendation via convolutional sequence embedding,” in *WSDM*, 2018, pp. 565–573.
- [38] N. Choudhary, N. Rao, S. Katariya, K. Subbian, and C. K. Reddy, “Probabilistic entity representation model for reasoning over knowledge graphs,” in *NeurIPS*, 2021, pp. 23 440–23 451.
- [39] F. Wang, Z. Zhang, L. Sun, J. Ye, and Y. Yan, “Dirie: Knowledge graph embedding with dirichlet distribution,” in *WWW*, 2022, pp. 3082–3091.
- [40] M. Li, X. Zhao, C. Lyu, M. Zhao, R. Wu, and R. Guo, “Mlp4rec: A pure MLP architecture for sequential recommendations,” in *IJCAI*, 2022, pp. 2138–2144.
- [41] R. He, W. Kang, and J. J. McAuley, “Translation-based recommendation,” in *RecSys*, 2017, pp. 161–169.
- [42] A. Said and A. Bellogin, “Comparative recommender system evaluation: benchmarking recommendation frameworks,” in *RecSys*, 2014, pp. 129–136.
- [43] D. P. Kingma and J. Ba, “Adam: A method for stochastic optimization,” in *ICLR*, 2015.
- [44] W. X. Zhao, Y. Hou, X. Pan, C. Yang, Z. Zhang, Z. Lin, J. Zhang, S. Bian, J. Tang, W. Sun, Y. Chen, L. Xu, G. Zhang, Z. Tian, C. Tian, S. Mu, X. Fan, X. Chen, and J. Wen, “Recbole 2.0: Towards a more up-to-date recommendation library,” in *CIKM*, 2022, pp. 4722–4726.
- [45] J. J. McAuley, C. Targett, Q. Shi, and A. van den Hengel, “Image-based recommendations on styles and substitutes,” in *SIGIR*, 2015, pp. 43–52.
- [46] Q. Bing, Q. Zhu, and Z. Dou, “Cognition-aware knowledge graph reasoning for explainable recommendation,” in *WSDM*, 2023, pp. 402–410.
- [47] X. Chen, Y. Zhang, and J. Wen, “Measuring “why” in recommender systems: a comprehensive survey on the evaluation of explainable recommendation,” in *IJCAI*, 2023.
- [48] Z. Wang, W. Zhang, N. Liu, and J. Wang, “Scalable rule-based representation learning for interpretable classification,” in *NeurIPS*, 2021, pp. 30 479–30 491.
- [49] —, “Learning interpretable rules for scalable data representation and classification,” *IEEE Trans. Pattern Anal. Mach. Intell.*, vol. 46, no. 2, pp. 1121–1133, 2024.